Dynamical Effects in Nuclear Collisions in the Fermi Energy Range : The Case of Heavy Systems

F. Bocage[1], J. Colin[1], M. Louvel[1], G. Auger[2], Ch.O. Bacri[3], N. Bellaize[1], B. Borderie[3], R. Bougault[1], R. Brou[1], P. Buchet[4], J.L. Charvet[4], A. Chbihi[2], D. Cussol[1], R. Dayras[4], N. De Cesare[7], A. Demeyer[5], D. Doré[4], D. Durand[1], J.D. Frankland[3], E. Galichet[5], E. Genouin-Duhamel[1], E. Gerlic[5], D. Guinet[5], P. Lautesse[5], J.L. Laville[2], J.F. Lecolley[1], R. Legrain[4], N. Le Neindre[1], O. Lopez[1], A.M. Maskay[5], L. Nalpas[4], A.D. Nguyen[1], M. Pârlog[6], J. Péter[1], E. Plagnol[3], M.F. Rivet[3], E. Rosato[7], F. Saint-Laurent[2,a], S. Salou[2], J.C. Steckmeyer[1], M. Stern[5], G. Tăbăcaru[6], B. Tamain[1], O. Tirel[2], L. Tassan-Got[3], E. Vient[1], M. Vigilante[7], C. Volant[4], J.P. Wieleczko[2],

(INDRA collaboration)

C. Le Brun[1], A. Genoux-Lubain[1,b], G. Rudolf [8], L. Stuttgé[8]

(NAUTILUS collaboration)

[1] LPC, IN2P3-CNRS, ISMRA et Université, F-14050 Caen Cedex, France.
[2] GANIL, CEA et IN2P3-CNRS, B.P. 5027, F-14076 Caen Cedex, France.
[3] Institut de Physique Nucléaire, IN2P3-CNRS, F-91406 Orsay Cedex, France.
[4] DAPNIA/SPhN, CEA/Saclay, F-91191 Gif sur Yvette Cedex, France.
[5] Institut de Physique Nucléaire, IN2P3-CNRS et Université, F-69622 Villeurbanne Cedex, France.
[6] National Institute for Physics and Nuclear Engineering, RO-76900 Bucharest-Măgurele, Romania.
[7] Dipartimento di Scienze Fisiche e Sezione INFN, Universiti Napoli "Federico II", I80126 Napoli, Italy.
[8] IRES(IN2P3-CNRS/Université Louis Pasteur) , 67037 Strasbourg Cedex, France.
a) present address: DRFC/STEP, CEA/Cadarache, F-13018 Saint-Paul-lez-Durance Cedex, France
b) present address: LPC Clermont-Ferrand, Université Blaise Pascal , 63177 Aubiere Cedex, France.

Abstract

Recent experimental results concerning heavy systems (Pb+Au, Pb+Ag, Pb+Al, Gd+C, Gd+U, Xe+Sn, ...) obtained at GANIL with the INDRA and NAUTILUS 4π arrays will be presented. The study of reaction mechanisms has shown the dominant binary and highly dissipative character of the process. The two heavy and excited fragments produced after the first stage of the interaction can experience various decay modes from evaporation to multifragmentation including fission.

However, deviations from this simple picture have been found by analysing angular and velocity distributions of light charged particles, and fragments. Indeed, there is an amount of matter in excess emitted between the two primary sources suggesting either the existence of a mid-rapidity source similar to the one observed in the relativistic regime (participants) or a strong deformation induced by the dynamics of the collision (neck instability). This last possibility has been suggested by analysing in detail the angular distributions of the fragments. More precisely, we observe an isotropic component which is compatible with the predictions of statistical models and a second one corresponding to breakup aligned on the recoil direction of the projectile like source which should be compared with the predictions of dynamical calculations based on microscopic transport models.

1 Introduction

Understanding the properties of nuclear matter is the most important challenge in nuclear physics. To achieve this goal, nuclei first have to be prepared in extreme conditions of excitation energy, temperature, pressure, spin and isospin. The tool used to obtain such extreme conditions is heavy ions induced reactions. For heavy systems in the Fermi energy range, two main primary fragments are formed after the collision : the primary projectile-like and the target-like fragments which can experience, depending on their excitation energies, various exit channels : evaporation of light particles, fission or multifragmentation.

To obtain physical information about the projectile-target nuclear interaction and the two excited primary fragments, the characteristics of all detected fragments and particles can be compared with those predicted by various models. For example, statistical models are often used [1, 5] to describe the decay of the primary fragments including "standard" fission. The comparison of experimental data with such models first implies to test whether all degrees of freedom are equilibrated (thermal, chemical and shape equilibrium) and whether there is no coupling left between entrance and exit channels . In this work, we present some results concerning one fixed exit channel : the breakup of the projectile-like source in two fragments for which we will give strong evidence for the occurrence of two types of mechanisms, namely standard fission and aligned breakup.

Before studying the projectile-like source breakup, we present an experimental method used to estimate the impact parameter of the collision (section 2) as well as an illustration about the binary aspect of the primary process (section 3). Next, the fission charge asymmetries obtained after collisions between a given projectile and different targets show strong reminiscences of the entrance channel (section 4). Moreover, angular distributions put forward privileged directions corresponding to aligned breakup which are incompatible with standard processes. In order to disentangle standard fission from aligned breakup a

method is then proposed, which allows to quantify the relative importance of these mechanisms as a function of the target and projectile sizes, the incident energy, the violence of the collision and the breakup asymmetry (section 5). We lastly study the differences between the characteristics of the two components and we compare the standard fission component with a statistical model in order to obtain information about the fissioning nucleus at the saddle point (section 6).

2 Experimental impact parameter

In Fig.1, the transverse energy of light charged particles $E_t^{12} = \sum E_i \sin^2(\theta_i)$ normalized to the available energy in the center of mass of the reaction E_{cm}^{avail} (where E_i is the kinetic energy of the particle i and θ_i its angle relative to the beam direction) is plotted for Xe+Sn system at different incident energies. The data presented here have been obtained with the minimal trigger condition to detect at least one charged product. Each curve is normalized to the corresponding total number of events and thus represents the transverse energy probability distribution.

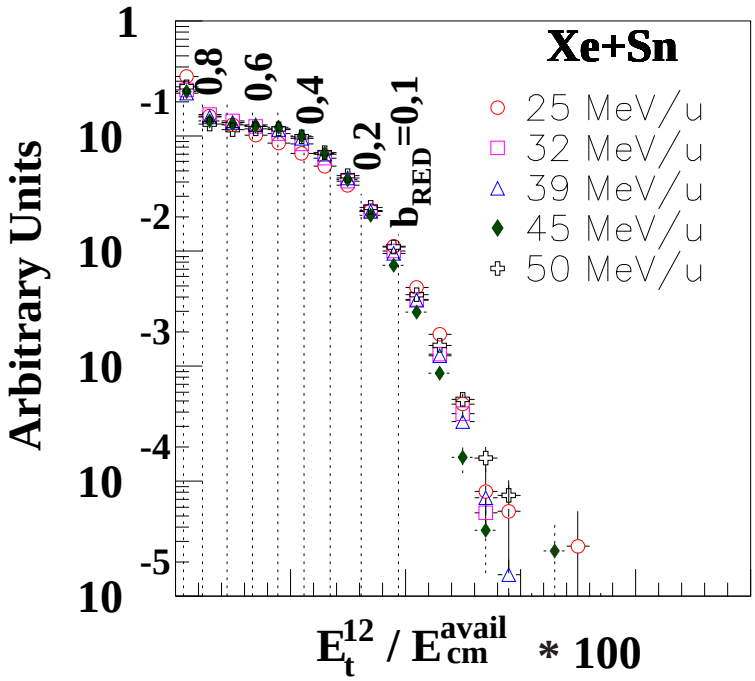

Figure 1: Transverse energy distributions for light charged particles with Z=1,2 divided by the available energy in the center of mass. The symbols correspond to various incident energies.

The distributions obtained at all the incident energies rather well superimpose on each other, in particular the maximum reached transverse energy corresponds to the same fraction of the available energy, whatever the incident energy. The same behaviour have already been observed with the requirement of four charged particles detected but shows more important trigger effects at low transverse energy[7]. This scaling with incident energies is expected for observables correlated to the impact parameter. Thus, an "experimental" impact parameter can be estimated by mean of these distributions [7, 9]: the impact parameter b is determined by assuming a geometrical correspondence between the cross section σ and the impact parameter ($\sigma = \pi b^2$) [10].

3 Reaction mechanisms

In Fig.2, the transverse versus parallel velocity invariant plots ($V_{par} - V_{per}$ correlations) for peripheral collisions are shown for protons, deuterons, tritons, alpha particles, and fragments with charge 3, 6, 10, 15 and 20.
For heavy systems at incident energies close to 30 MeV/u, most of the collisions correspond to binary processes [11], [12]. We observe two nice circles around the projectile and target parallel velocities ($|V_{par}| = 4.5\ cm/ns$), except for some reaction products emitted by the target which are too slow to be detected or identified. Also we can see an amount of matter in excess between the two reaction partners. To go into detail, we have plotted on Fig.3 the parallel velocity distributions of the particles and fragments (light grey area) coincidentally detected with a projectile-like residue (dark grey area) defined as the heaviest fragment. For all particles and fragments, we observe that the forward part ($V_{//} > V_{PLF}$) of the velocity distributions (not influenced by threshold effects) are not symmetrical with respect to the projectile-like residue velocity. A large number of fragments and light charged particles are emitted between the two reaction partners. Such a behaviour suggested to us to study the fragment production against their size by means of angular correlations. The mid-rapidity particles and fragments have already been studied in different works [12, 19] and in this paper we focus our studies on fragments emitted by the PLF which correspond mainly to the plots of the lower rows in Fig.2 and Fig.3.

4 Influence of the entrance channel on the PLF binary breakup

We will now study the binary breakup of the PLF for various systems and incident energies. In this purpose we select the events with two fragments emitted forward in the center of mass and assume that these two fragments result from the binary breakup of the PLF.

We first present in Fig.4 the charge asymmetry distributions of the two fragments

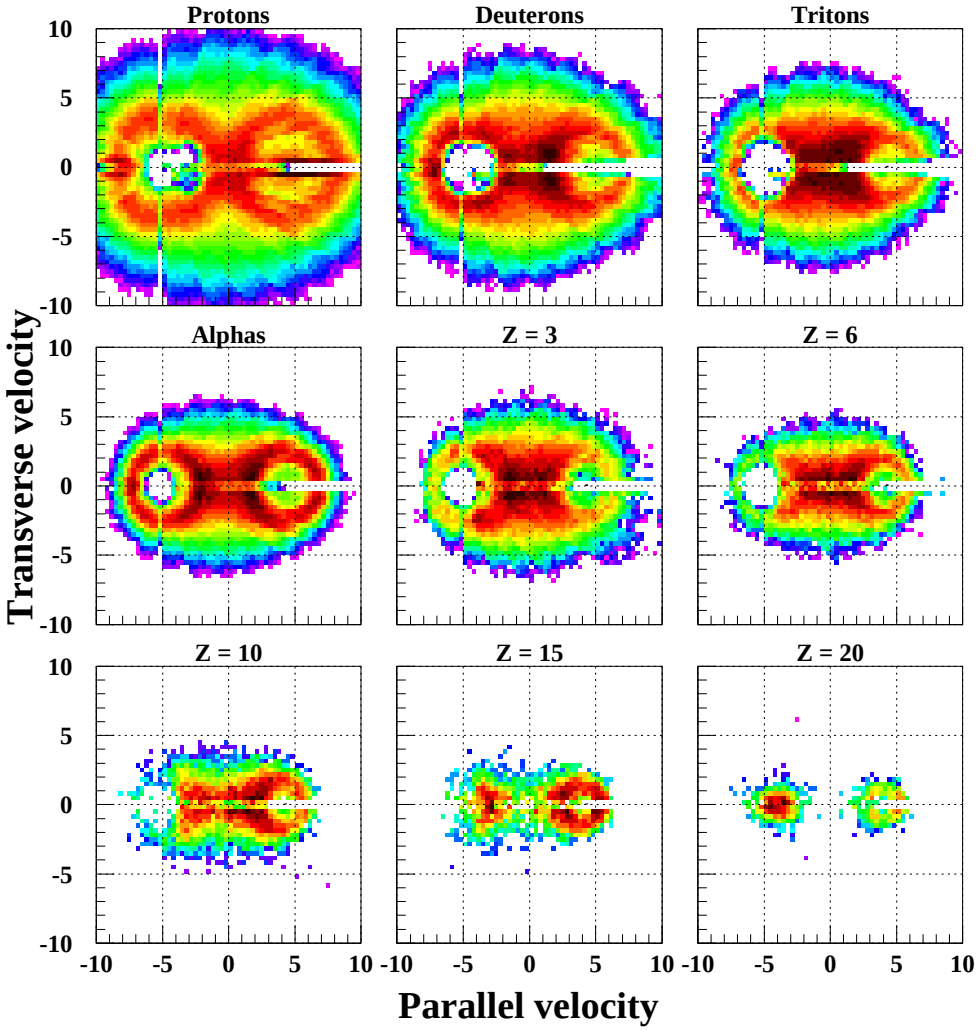

Figure 2: Vpar-Vper (cm/ns) invariant velocity plots, in the center of mass, for the Xe+Sn system at 45 MeV/u for peripheral collisions. The different panels present various types of reaction products : light charged particles (p,d,t,α) and fragments with charge 3, 6, 10, 15 and 20.

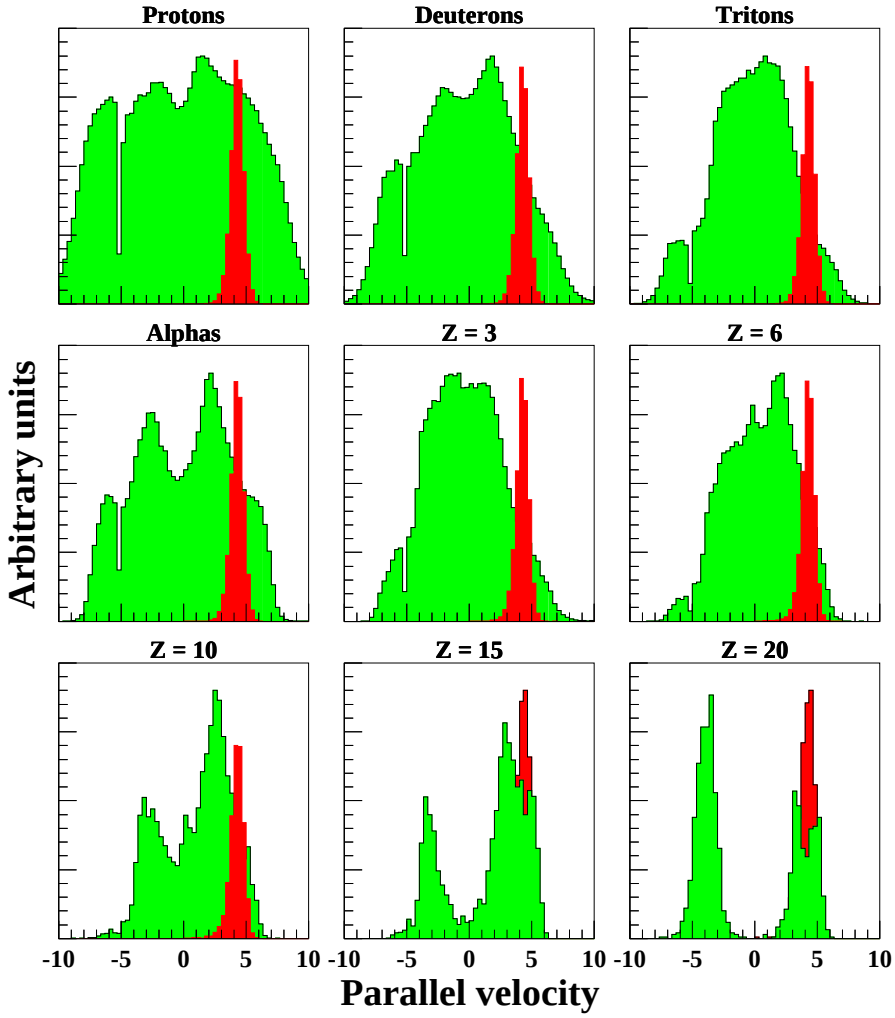

Figure 3: Xe+Sn system at 45 MeV/u, peripheral collisions : parallel velocity distributions (cm/ns) for the same type of reaction products as in Fig.2 (light grey area) and for the heaviest fragment detected in coincidence (dark grey area).

$\eta = |(Z_1 - Z_2)|/(Z_1 + Z_2)$ for different projectile-targets combinations . For light targets (carbon or aluminum) the breakup is mainly symmetrical ($\eta = 0$) in accordance with the expectation for the statistical fission of a heavy nucleus. For the heaviest targets the breakup of the PLF shows in addition an important contribution for the highest asymmetries. This additional component increases with the size of the target. On the contrary to what is observed for the fission of a heavy projectile-like fragment which only depends, in the case of standart fission, on the exit channel parameters (excitation energy, angular momentum, ...), the breakup of the PLF here depends strongly on the target size which is a characteristic of the entrance channel.

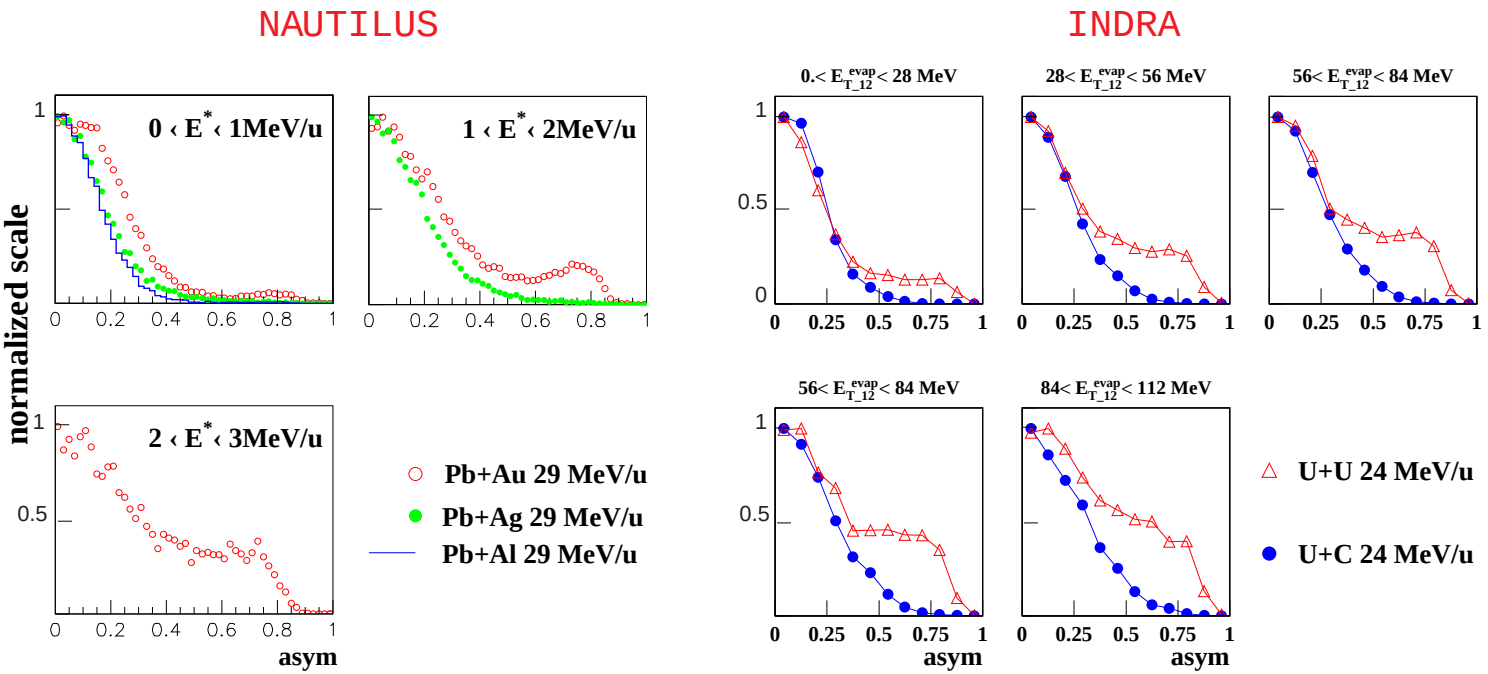

Figure 4: Left part: Asymmetry distribution for fission fragments of a lead projectile-like fragment after a collision with a gold target (open circles), a silver target (full circles), or a aluminum target (line). Right part: Asymmetry distributions for fission fragments of a uranium projectile-like fragment after a collision with a uranium target (open triangles) or a carbon target (full circles). These distributions are arbitrary normalised at $\eta = 0$.

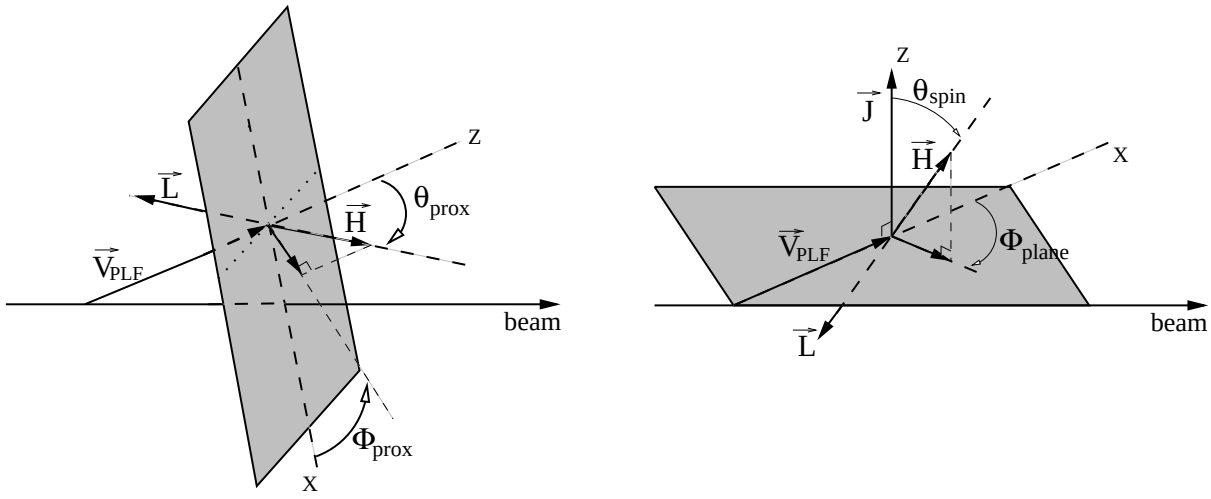

Figure 5: Left panel: θ_{prox} definition : angle between the breakup axis, orientated from the light L to the heavy fragment H, and the recoil velocity in the center of mass of the projectile-like fragment (noted V_{PLF}) reconstructed with the two fission fragments. Right panel: θ_{spin} definition : angle between the fission axis oriented towards the heaviest fission fragment H and the reaction plane deduced from the recoil velocity of the projectile like fragment (labelled V_{PLF}) and the beam velocity. ϕ_{plane} definition : angle between the fission axis projected on the reaction plane and the recoil velocity of the projectile like fragment .

To understand such an effect, the angular distributions of the fragments are studied. In this purpose, we reconstruct the PLF, its velocity, its breakup axis (the axis between the two detected fragments) and also the reaction plane, defined by the recoil direction of the PLF and the beam axis. In order to take into account the influence of the size of the two fragments, observed in Fig.2 and Fig.3, this axis is oriented from the light to the heavy fragment (Fig.5).

The "proximity angle" θ_{prox} is the angle between the direction of the PLF velocity and the breakup axis (see Fig.5). In the case of a standard fission, all directions are allowed and a symmetrical flat distribution with respect to zero is expected. Spin effect, if any, favours the reaction plane, thus the recoil axis, and then increases slightly and symmetrically the distribution for $\cos(\theta_{prox}) = \pm 1$. In Fig.6, we present the experimental $\cos(\theta_{prox})$ distributions associated with the PLF breakup for Pb and Gd projectiles impinging on different targets (Al, C, Ag, AU and U) for different breakup asymmetries η. We observe that for the lightest targets (Al, C), the distributions obtained are symmetrical with respect to zero as expected in standard fission of a rotating nucleus. For some final configurations, detection effects lead to a depletion at $\cos(\theta_{prox}) = \pm 1$. These angles would correspond to a binary breakup aligned with the PLF recoil axis and thus to a detection of the two fragments in the same detector. These configurations are rejected. For the Ag target, for symmetrical breakup the distribution is compatible with a standard fission; for

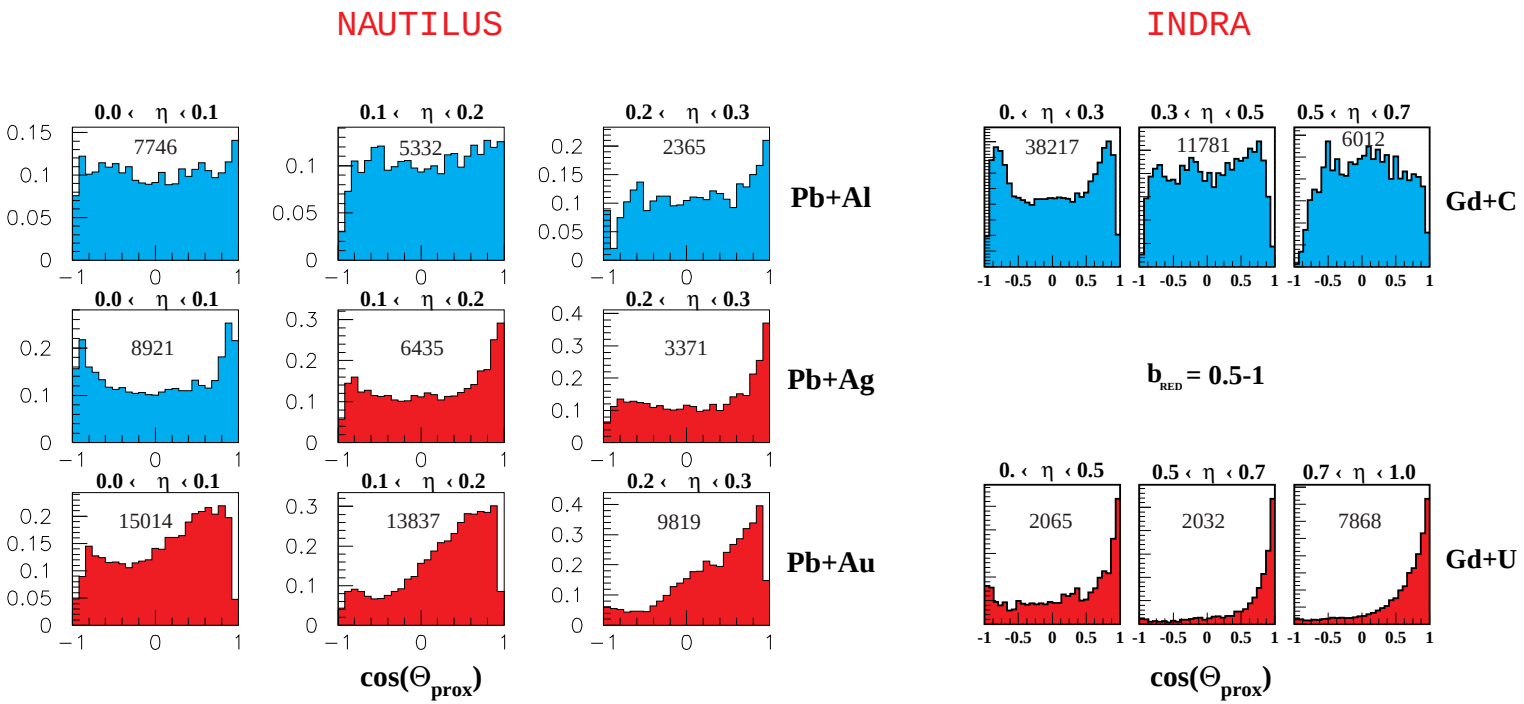

Figure 6: Pb+Al, Ag, Au at 29 MeV/u (NAUTILUS) and Gd+C, U at 36 MeV/u (INDRA) for peripheral collisions.
cos (θ_{prox}) distributions associated with the fission of the PLF for different targets (rows) and for different fission asymmetries (columns) . The light gray distributions are compatible with standart fissions processes and the dark gray distributions correspond to the addition of two components, a standart and an aligned one. The number of experimental events is indicated in each box.

asymmetrical breakup (η >0.2), the distributions are peaked at $\cos(\theta_{prox}) = +1$ which corresponds to a breakup aligned on the PLF recoil axis, with the heavy fragment faster than the light one. For the Au and U targets the asymmetrical distributions are observed even for the smallest breakup asymmetries.
Thus, for heavier targets and greater asymmetries, the breakup axis is preferentially aligned with the separation direction of the two primary fragments (TLF and PLF), the lighter fragment emitted by the PLF being located between the heavy one and the TLF. This effect increases with the size of the target and the asymmetry of the PLF breakup. Like the charge asymmetry distributions, this privileged direction depending on the charges of the PLF fragments, suggests to us a target effect. Such a behaviour can not be understood in a classical approach of standard fission because this statistical description presupposes that there is no coupling left between entrance and exit channels. The only privileged directions compatible with this description are the reaction plane due to spin effects, and the plane perpendicular to the PLF-TLF separation direction due to Coulomb repulsion [20], [21]. The alignement that we observed thus suggests the breakup of a deformed projectile-like source on the recoil axis. Aligned binary breakup of the PLF has been previously observed at Fermi energies [13], [22], and also at lower energies [20], [23], [24].

5 Competition between fission and aligned breakup

5.1 Separation of the two contributions with angular distributions

The distributions plotted in Fig.6, can be viewed as the sum of two components : the first one, symmetrical with respect to $\cos(\theta_{prox}) = 0$, could be associated to standard fission, and the second one peaked at $\cos(\theta_{prox}) = 1$ to aligned breakup. For a given projectile, the relative weights of these two components depend on the target size and the breakup asymmetry. In order to isolate the first component, we symmetrized around $\cos(\theta_{prox}) = 0$ the backward part ($cos(\theta_{prox}) < 0$) of the experimental distribution, supposing thus that this part is not influenced by non-statistical breakup : the $cos(\theta_{prox})$ distribution are indeed expected to be symmetrical in the case of standard fission. The aligned contribution is then obtained by subtracting this standard fission distribution from the total experimental distribution. The result of this procedure is shown in the central column of Fig.7, whereas the initial distributions are presented in the left one, for different breakup asymmetries of Pb impinging on Ag target. The percentage of aligned breakup for each asymmetry is given in the central column of Fig.7. This percentage increases with the asymmetry from 5% ($\eta = 0 - 0.1$) to 22% ($\eta = 0.3 - 0.4$) which corresponds to a charge value of 54 for the heaviest fragment and 26 for the lightest one.
Definding θ_{spin} as the angle between the breakup axis and the aligned spin axis (Fig.5), we have plotted the $\cos(\theta_{spin})$ distributions in the last column of Fig.7. The higher the

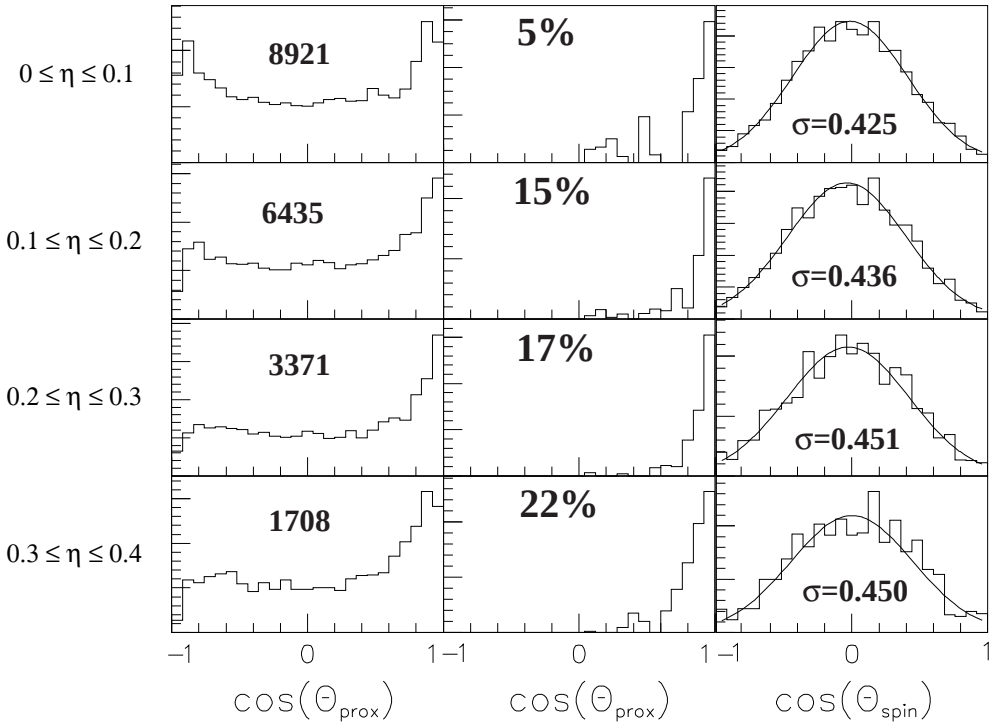

Figure 7: Pb + Ag at 29 MeV/u for peripheral collisions (NAUTILUS). Left panel : $\cos(\theta_{prox})$ distributions associated with different fission asymmetries. The number of experimental events is indicated in each box. Central panel : $\cos(\theta_{prox})$ distributions obtained after substraction of the reconstructed standard fission distribution from the total distribution. The percentage of aligned fission relative to the total events for the same asymmetry is given on each panel (see text for details). Right panel : $\cos(\theta_{spin})$ distributions associated with different fission asymmetries (see text for the θ_{spin} definition).

value of the spin of the fissioning nucleus, the more the fission fragments are emitted in the reaction plane. Furthermore, the breakup aligned with the PLF recoil axis also favour the reaction plane. Both mecanisms contribute to the "bell shape" curve obtained in the last column of Fig.7 (the reaction plane corresponds to $\cos\theta_{spin} = 0$) and their relative contributions are difficult to estimate. When the probability of aligned breakup is relatively low, spin effects dominate: the width of the $\cos\theta_{spin}$ distributions, often used to measure the angular momentum of the fissioning nucleus [25], will then give only slightly overestimated spin values.

When the aligned breakup become dominant, the couple of angles (θ_{spin}, θ_{prox}) does not allow to measure the angular momentum of the fissioning nuclei, because these two angles are not independent. It is more appropriate to use another angle, ϕ_{plane}, defined as the angle between the breakup axis projected on the reaction plane and the recoil velocity of the PLF (see Fig.5). The two angles θ_{spin} and ϕ_{plane} belong to spherical coordinates in

the PLF frame and thus are independent.

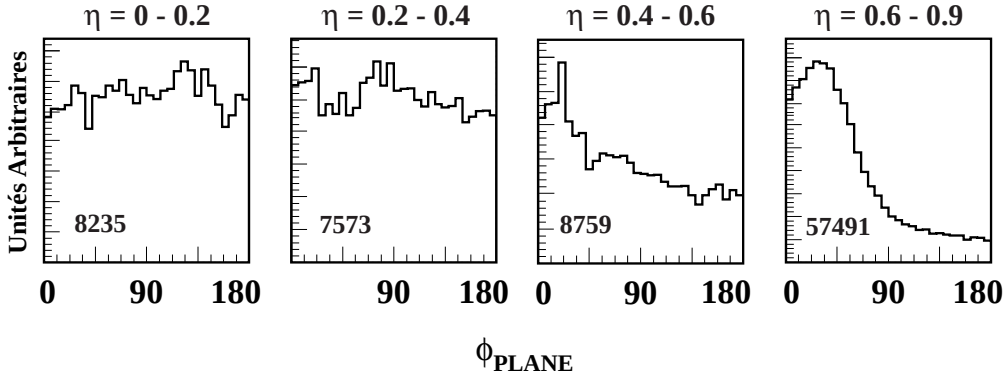

Figure 8: Xe+Sn system at 25 MeV/u. ϕ_{plane} angle distributions for different values of the fission asymmetry and for peripheral events (b_{RED}=0.8-1.). The number of experimental events is indicated in each box.

For a standard fission, a ϕ_{plane} distribution is expected to be flat even with spin effects. Fig.8 presents such distributions for Xe+Sn at 25 MeV/u for the most peripheral events. For symmetrical breakup (left plot on Fig.8), the ϕ_{plane} distribution is roughly flat in agreement with the expectations of a standard fission, but for asymmetrical breakup (right plot on Fig.8), a large contribution emerges for small values of ϕ_{plane}, associated with aligned breakup.

We can select the events associated with the flat part of the ϕ_{plane} distribution. Like those lying in the backward part of the $cos(\theta_{prox})$ distributions, these events may be considered as standard fission of PLFs. Since the ϕ_{plane} distributions are not influenced by spin effects, the flat part of the ϕ_{plane} distribution is representative of the whole standard fission component. We can use the $cos(\theta_{spin})$ distributions associated with the flat part of the ϕ_{plane} distribution to estimate the angular momentum of the projectile-like fragments which experience standard fission (see section 6). We should first of all select events compatible with statistical assumptions before extracting any physical information from comparisons with statistical models.

5.2 Probabilities associated with the two contributions

The probabilities of standard fission and aligned breakup are presented (Fig.9) against the breakup asymmetry for the Xe+Sn system at various incident energies and for several impact parameters. We first observe that the probabilities of both types of breakup do not depend on the incident energy. While the asymmetry distributions of statistical fission slightly change with the impact parameter, those of aligned breakup become broader from peripheral to central collisions. So it seems that the violence of the collision influences more the aligned breakup than the statistical fission.

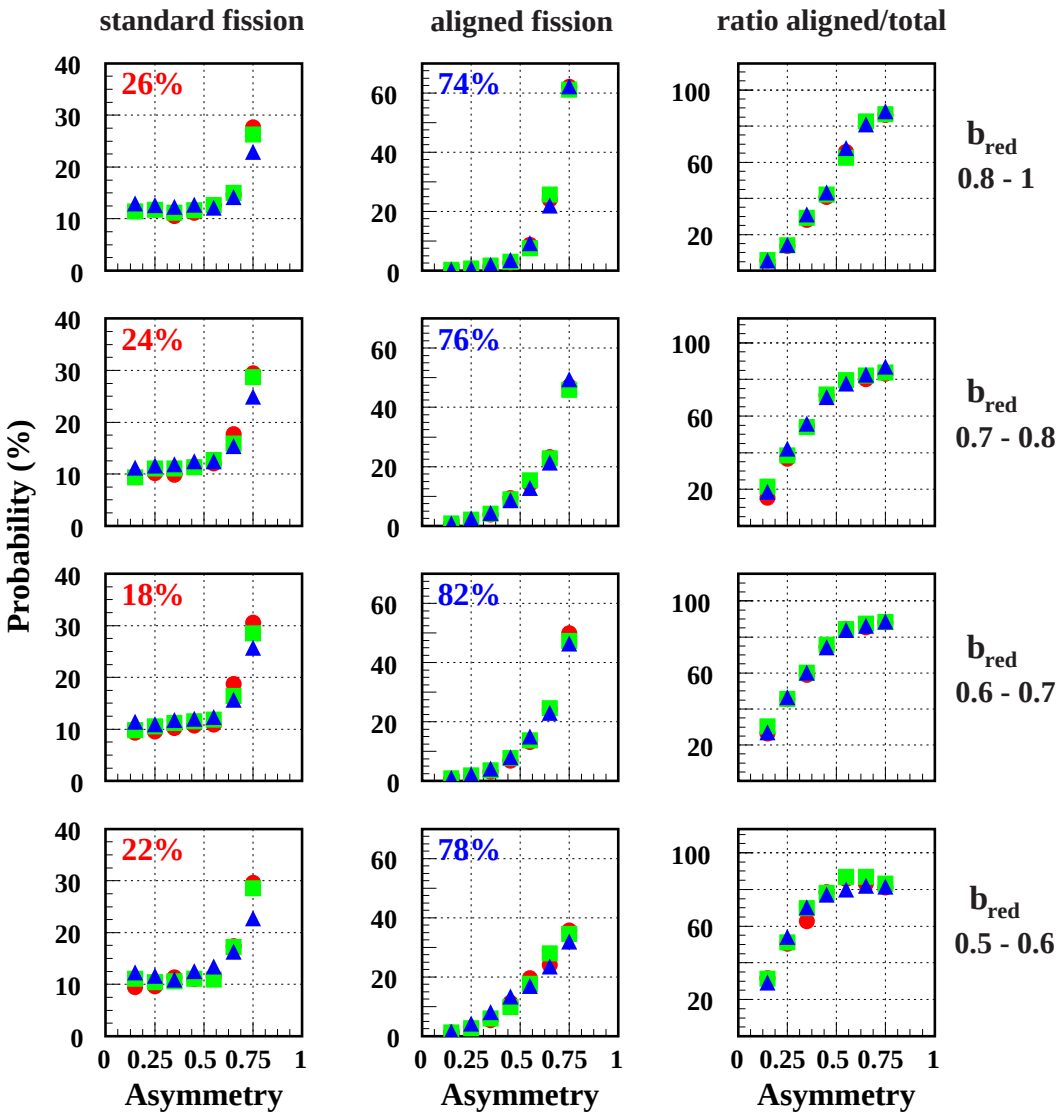

Figure 9: Asymmetry distribution against breakup asymmetry associated with standard fission (left column) and with aligned breakup (central column) for the Xe+Sn systems at various incident energies (circles 50 MeV/u, squares 45 MeV/u, triangles 39 MeV/u) and for several impact parameters. The third column presents in addition the proportion of aligned breakup against charge asymmetry. The different rows correspond to different impact parameter bins.

Moreover, the third column of Fig.9, presenting the proportion of aligned breakup against the charge asymmetry, show that aligned breakup become more and more likely with increasing asymmetry and with decreasing impact parameter.

For this system, the standard fission represents only 25% of the total number of events whatever the incident energy and impact parameter. In the case of Pb+Ag, for roughly the

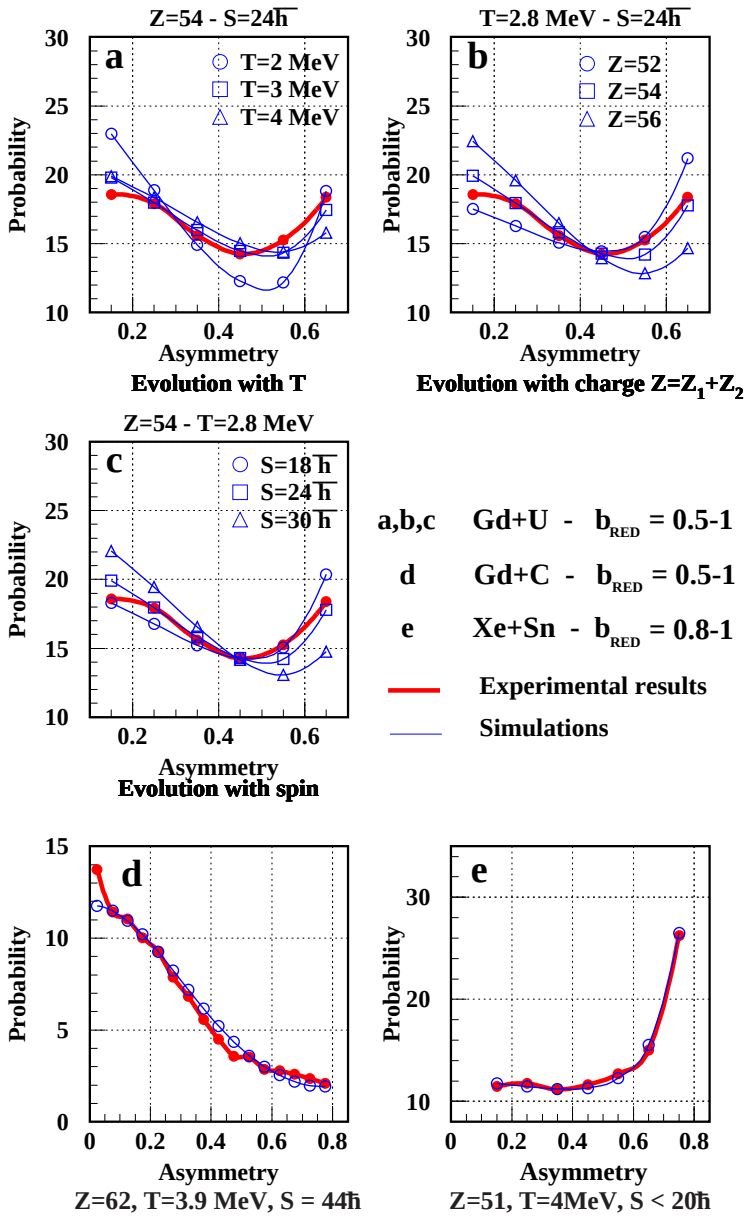

Figure 10: Standard fission probability against breakup asymmetry for different systems and impact parameters integrated from b_{max} (peripheral collisions) to $0.5b_{max}$ for the Gd+U system at 36 MeV/u (a,b,c). evolution with: a: the temperature of the fissioning nucleus. b : charge of the fissioning nucleus. c: spin of the fissioning nucleus. d: Gd+C system at 36 MeV/u. e: Xe+Sn system at 45 MeV/u. The full symbols correspond to the data, the open symbols to the calculations.

same target than Xe+Sn, the standard fission integrated over asymmetry represents 85% of the total number of events. This difference between Xe+Sn and Pb+Ag system is due

to the fissility of the two projectiles. Depending on the studied systems, aligned breakup can be the dominant process and the physical information, like fission probabilities or angular momentum, obtained with such models would certainly be wrong [28]. So it is very important to first separate the events associated with standard fission in order to compare them to statistical models predictions.

6 Comparisons with a statistical prescription

The methods used to quantify the two mechanisms are entirely based on the reasonable assumption that the backward part of the $cos(\theta_{prox})$ distributions, or the flat part of the ϕ_{plane} distributions, are compatible with the statistical description and thus correspond to standard fission. Now we want to verify that the asymmetry distribution of these events are indeed compatible with a statistical prescription. These asymmetry distributions have been compared to those predicted by the "transition state model" [2], [29] with the fission barrier values given in [30]. This model calculates the probability of observing a given fission asymmetry for a fixed charge of the fissioning nucleus, a fixed temperature and a fixed angular momentum. It is applied to different systems Gd+U, Gd+C and Xe+Sn (Fig.10).

We have some constraints on the "free" parameters. The $\cos(\theta_{spin})$ distributions, associated with the flat part of the ϕ_{plane} distributions (method presented in section 5.1), give us a constraint on the ratio $J/\sqrt{T}$ [25]. Moreover, the charge of the fissioning nucleus is necessarily greater than or equal to the sum of the charges of the two detected fragments. For the Gd+U system at 36MeV/u, the shape of the curve is very sensitive to the "free" parameters (charge, temperature and spin of the fissioning nuclei). For example we can see a large difference when the temperature is increased from 2 to 3 MeV (Fig.10a). The results of our comparison show that the experimental asymmetry distribution is compatible with the calculated one for the fissioning nucleus at the saddle point with charge 54, temperature 3 MeV and spin $24\hbar$. The uncertainty of these values can be estimated from Fig 10 a-c. The charge 54 is equal to the sum of the charges of the detected fission fragments. So it suggests that the fission process takes place at the very end of the decay process [26], [27].

Although the variations of the breakup probabilities with asymmetry are very different for the three studied PLFs, they are rather well reproduced by the calculation with reasonable values for the charge, the temperature and the spin of the fissioning nuclei.

These different asymmetry distributions reflect the fissility of the studied fissioning nucleus. The statistical fission are mainly symmetrical for heavy PLF with a high fissility (distribution obtained for Gd+C with $Z_{PLF} = 62$) and mainly asymmetrical for light PLF with lower fissibility. The disappearance of a maximum at $\eta = 0$ in the asymmetry distribution is known as the Businaro-Gallone point. The distribution obtained for Xe+Sn with $Z_{PLF} = 51$ corresponds to this situation. This result is in agreement with the predicted mass rage$A_{BG} = 81 - 145$ [30] and the observed one $A_{BG} = 100$ [31]. The agreement with statistical model predictions for various PLFs can be considered as a solid proof of the

validity of our method to separate statistical fission and aligned breakup : all variables associated with the first type of events are rather well reproduced by statistical models.

Lastly we studied the relative velocity between the two fission fragments of the PLF. We compare the values obtained for the experimental standard fission with the prediction of a crude calculation using the Coulomb repulsion (equation 1) and also with the values obtained for the aligned breakup in order to extract some quantitative information on this last process (Fig.11). The contribution of aligned breakup to the relative velocity distribution is obtained by subtracting the contribution associated with the standard fission from the total relative velocity distribution. The lines correspond to the value of relative velocities obtained with the equations 1 and 2 (dark lines Fig.11).

$$E_C = 1.44 \frac{Z_1 Z_2}{R_1 + R_2 + 2} \tag{1}$$

$$V_{REL}/c = \sqrt{\frac{2 * E_C}{\mu c^2}} \tag{2}$$

Where E_C is the Coulomb energy between the fission fragments, Z_1, Z_2, R_1, R_2, μ the charges, radius and the reduce mass of the two fission fragments.

For symmetrical fission ($\eta = 0.$), the relative velocity obtained with these equations is 2.20 cm/ns. This value is compatible with the Viola sytematic [32]. To take into account the thermal energy (T=4MeV) estimated from the asymmetry distribution Fig.10.e, we have added arbitrary 2T in the previous calculation (grey lines Fig.11).

Except for the highest asymmetries ($\eta > 0.5$) and the lowest impact parameters, the velocities remains roughly compatible with the calculation for the most part of the standard fission component (Fig.11a). On the contrary, in Fig.11b, the relative velocity values are always higher for the aligned component. Even for peripheral events the relative velocities are higher than those obtained with the calculation. They also show a strong evolution with the impact parameter, mainly for the symmetrical fission. For the standard fission the deviations between data and the calculation can be understood by a little mixing between standard and aligned fission becausse for the highest asymmetries the aligned component dominates and the separation is difficult.

All these observations suggest that the aligned fission originates from very strong deformations of the projectile during its interaction with the target. Just after the collision the deformation is so large that the projectile-like fragment goes inevitably towards breakup: the PLF does not return to his equilibrated shape before its breakup, like in the case of a standard fission. Its deformation is as large (or even more) as the deformation of the same nucleus at the saddle point in a standard fission process. The process is continuous, so the relative velocity associated to the deformation at the saddle point is

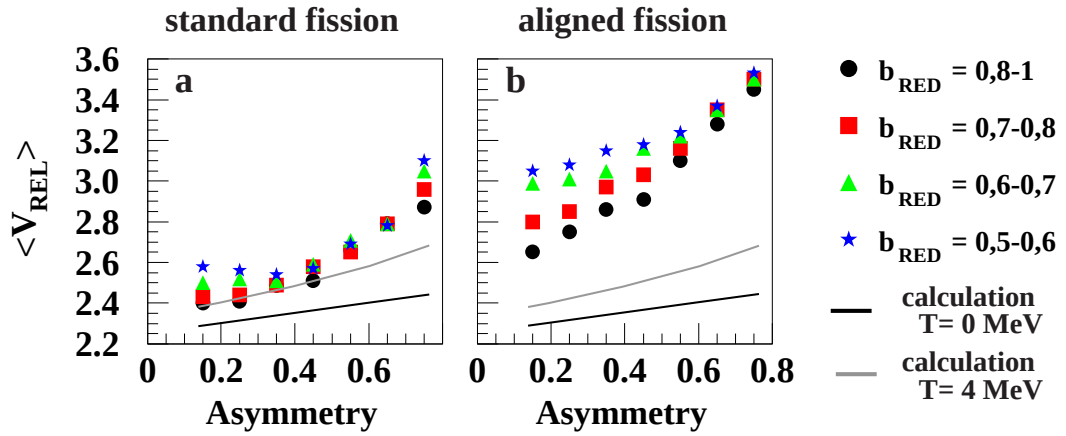

Figure 11: Relative velocities (cm/ns) against fission asymmetry for different impact parameters for the Xe+Sn at 45MeV/u. The full symbols correspond to mean values. Left column: distribution associated with the standard fission. Right column: distribution associated with the aligned component. The lines correspond to different values of the temperature 0MeV(dark line), 4MeV(grey line) add to the Coulomb repulsion(see text and equations 1 and 2 for details).

different from zero. This velocity can be considered as a deformation velocity which is related to the viscosity of nuclear matter. Thus, the measured relative velocity between the fission fragments is higher than in a standard fission. This observed relative velocity is the addition of the Coulomb repulsion and the deformation velocity of the PLF, and then puts an experimental constraint on nuclear viscosity.

7 Summary

We first have given evidence for the binary aspect of the collisions but also for different origins of particles and fragments. In this work we focused our study on the decay in two fragments of the projectile-like source. By using all informations obtained with 4π arrays, not only the global observables but mainly the correlated observables like angular distributions, asymmetry and relative velocity distributions of the fission fragments, two breakup mecanisms could be identified. The angular and charge asymmetry distributions of the one component are compatible with standard fission ; the comparison of these events with calculations based on statistical hypothesis allows us to obtain the characteristics of the fissioning nucleus the charge, the temperature and the spin at the saddle point. Moreover, the measured relative velocities between the two fission fragments are rather well reproduced with a Coulomb repulsion velocity.

The other component corresponds mainly to breakup aligned on the recoil velocity of the projectile-like source and become more and more likely for heavier target and more violent collisions. These evolutions coupled to very hight relative velocities which depend

on the impact parameter, indicate a strong reminiscence of the entrance channel in this particular exit channel. Such a coupling is inconsistent with statistical hypothesis and these events, which represent up to 75% of the binary breakup events for the Xe+Sn system, should be compared with dynamical calculations.

References

[1] Weisskopff et al., Physical Review C52 (1937) 295

[2] N. Bohr et al., Physical Review 56 (1939) 426

[3] L.G. Moretto et al., Physical Review Letters 74 N9 (1995) 1530

[4] L.G. Moretto et al., Physics Reports 287 (1997) 249

[5] K. Tso et al., Physical Letters B361 (1995) 25-30

[6] R.J. Charity et al., Nuclear Physics A483 (1988) 371

[7] E. Plagnol et al., Preprint IPNO DR 99-10, Phys.Rev. C (in press)

[8] J. Peter et al., Nuclear Physics A519 (1990) 611

[9] L. Phair et al., Nuclear Physics A548 (1992) 489

[10] C. Cavata et al., Physical Review C42 N4 (1990) 1760

[11] J.F. Lecolley et al., Physics Letters B325 (1994) 317

[12] V. Métivier Thèse Université de Caen (1995)
V. Métivier et al., Nuclear Physics A (in press)

[13] C.P. Montoya et al., Physical Review Letters 73 (1994) 3070

[14] W.G. Lynch, Nuclear Physics A583 (1995) 471

[15] T. Lefort et al. (INDRA collaboration), Preprint LPCC 98-15, Nuclear Physics A (in press)

[16] D.Doré et al. (INDRA collaboration), Proceedings of the XXXVIth Winter Meeting on Nuclear Physics, Edited by I.Iori, 26-31 January 1998, Bormio, Italy, 381-394.

[17] E. Galichet et al. (INDRA collaboration), Proceedings of the XXXVIth Winter Meeting on Nuclear Physics, Edited by I.Iori, 26-31 January 1998, Bormio, Italy, 410-424.

[18] J. Lukasik et al., Physical Review C vol. 55, Num. 4 (1997)

[19] O. Tirel Thèse Université de Caen (1998)

[20] P. Glassel et al., Z. Phys. A310 (1983) 189

[21] D. Durand et al., Physics Letters B345 (1995) 397

[22] J.F. Lecolley et al., Physics Letters B354 (1995) 202

[23] G. Casini et al., Phys. Rev. Lett., 71-16 (1993) 2567

[24] A.A. Stefanini et al., Zeitschrift Physik A351 (1995)167

[25] J. Colin et al., Nuclear Physics A593 (1995) 48

[26] D.J. Hinde et al., Nuclear Physics A452 (1986) 550
D.J. Hinde et al., Nuclear Physics A538 (1992) 243c

[27] D. Hilcher et al., Phys. Rev. Letters vol 62 (1989) 1099

[28] J.C. Steckmeyer, Proceedings of the XXXVIIth Winter Meeting on Nuclear Physics, Edited by I.Iori, 25-30 January 1999, Bormio, Italy, 230-240.

[29] L.G. Moretto et al., Nuclear Physics A274 (1975) 211

[30] G. Royer et al., Nuclear Physics A466 (1987) 139;
G. Royer et al., Journal of physics G20 (1994) L131;
G. Royer, F. Haddad Journal of physics G21 (1995) 339

[31] L.G. Sobotka et al.,Phys. Rev. Letters vol 53 (1984) 2004

[32] V.E. Viola et al.,Physical Review C31 (1985) 1550